Journal of Geomatics Vol. 18, No. 2, October 2024

Comparative Use of UAV and Satellite Images in Discrimination and Estimation of Cashew Plantation Areas

Alain Abi-Kabérou[1], Lambert Zountchegnon[2], Jean-Paul Rudant[3] and Bruno Djossa[1]
[1]Université Nationale d'Agriculture, Benin, [2]Université de Parakou, Benin, [3]Université Gustave Eiffel, ENSG, IGN, France
*Email : abisadock20@gmail.com

(Received on 7 Feburary, 2024; in final form 12 September 2024)

***DOI**: https://doi.org/10.58825/jog.2024.18.2.147*

Abstract: Cashew plantations generate significant interest in Benin due to their high socioeconomic value for the population. A thorough understanding of the spatial distribution of these plantations is crucial for comprehending their environmental and socioeconomic impacts. In this study, various types of multi-sensor imagery were compared to assess each sensor's capabilities in mapping plantation areas. The study was conducted in the Savè commune, a major industrial cashew-producing region. Multispectral sensors from Landsat-8 Operational Land Imager (OLI), Sentinel-2A, and UAV multispectral platforms, along with ground surveys, were fused and classified using the Random Forest algorithm. The study results allowed for the assessment of uncertainties associated with different platforms in detecting cashew plantations in the test area. Classification using Random Forest algorithms on UAV, Sentinel, and Landsat platform images yielded overall accuracies of 83%, 65%, and 48%, respectively. Producer and user accuracies were 94% and 75% for the UAV platform, 98% and 71% for the Sentinel platform, and 91% and 77% for the Landsat platform in cashew tree detection. This study demonstrates the complementarity among various platforms in detecting and mapping cashew plantations.

Keywords : cashew plantations ; UAV ; Landsat ; Sentinel-2; Random Forest; data fusion.

1. Introduction

The cashew tree is a cash and export crop of significant importance in West African countries, including Benin. In Benin, cashew ranks as the second agricultural export product after cotton. Cashew nut exports have experienced substantial growth, increasing from 36,487 tons of raw nuts in 2001 (PAC/DCM/SESP, 2009) to 146,332 tons in 2011 (ACA 2012). Cashew represents 8% of the total export value in 2008, contributing to 7% of the agricultural GDP and 3% of the national GDP (Tandjiékpon 2010).

However, the lack of accurate and precise information on forest resources poses a significant obstacle to adaptive and effective plantation management, hindering timely decision-making. Two crucial needs arise to address this challenge: firstly, the development of precise inventory systems that spatially assess plantation occupancy and other ecosystem services related to the plantation; secondly, promoting the use of these systems to improve carbon stock modeling by these ecosystems. The challenge faced by managers is to ensure integrated and sustainable management of these ecosystems. To address these conflicting expectations, forest managers require comprehensive, precise, geolocated, up-to-date, and cost-effective information. Forest inventories primarily aim at planning management units (Power and Gillis 2006) and serve multiple resource management objectives. However, the spatial resolution and attributes of polygons interpreted from conventional photographs are often insufficient to support planning, management, and investment decisions necessary for improving the competitiveness of the forestry sector (Queinnec et al. 2021).

There is limited knowledge and information on the distribution and status of plantations in Africa to support public policies in this domain. Currently, there is no regional plantation database, and envisioning such mapping using traditional field techniques is impractical. Spatializing these plantations is crucial for accurate resource estimation. Previous inventories relied on survey and point measurement techniques with drawbacks such as slow and costly implementation, difficulties in tracking evolving phenomena, and proven effectiveness over at least a quarter of a century (Saadou 1999). Moreover, forest plantation ecosystems play a key role in mitigating the adverse effects of climate change by absorbing carbon dioxide, a major greenhouse gas responsible for global warming. In Benin, knowledge about the biomass produced by this species is very limited. However, woody biomass provides valuable insights into the ecological and economic productivity of agroecosystems (Kémeuzé et al. 2012).

In forestry, a sensor's spatial resolution largely determines its utility for resource estimation. The main factors to consider are the nominal size of production units (production area, conservation area, agricultural land) and mappable topographical features (tree cover, mixed crops, and valid land use elements) that play a role in statistical estimates. However, satellite imagery seems promising for providing certain information requested by current and potential cashew producers, as well as forestry administration data. Generally, small areas are easier to study with high-resolution images due to the technical

capabilities of sensors to acquire timely images and lower associated costs.

Drone and satellite systems have complementary features. This complementarity is even stronger with environmental monitoring satellites, providing highly accessible data and an observational scale complementary to drones (Alvarez-Vanhard et al. 2021). On one hand, satellites cover large territories with periodic observations, while, on the other hand, drones provide a cost-effective solution to specify satellite observations with their Very High Spatial Resolution (VHSR) sensors and acquisition flexibility. However, the swath of UAV images depends on the flight altitude and directly influences image resolution, footprint, and the number of images needed to cover a study area at a given image overlap (Lisein et al. 2015). Drones have the disadvantage of having a smaller swath (a few km²), often due to their low energy reserves and regulations concerning safety and privacy. Therefore, for optimal altitude, a compromise between resolution and the maximum scanned area is required; lower flight altitudes result in higher image resolution and smaller scanned areas. On the other hand, the swath of low-resolution satellite sensors is much larger. MODIS (Moderate-Resolution Imaging Spectro radiometer) can cover up to 2,100 km. However, these images cannot capture topographic details to delineate production areas. Furthermore, each drone and satellite system have specific acquisition characteristics resulting from a compromise between resolutions (spatial, spectral, and temporal), swath, and signal-to-noise ratio (Alavipanah et al. 2010).

The complementarities of scales have already been studied between satellite and/or airborne systems (Alvarez-Vanhard et al. 2021; Zhang 2010), but few studies focus on evaluating these different technologies in estimating plantation areas, which show an interesting potential for synergies. In this study, we will analyze the capacity of different platforms (satellite and UAV) using a multi-sensor approach with new remote sensing technologies (UAV, Sentinel, and Landsat) to propose a suitable methodology for delineating plots and characterizing forest plantations, facilitating the calculation of cashew plantation areas. To achieve this, we used data from various satellite platforms (Sentinel-2A and Landsat 8 OLI) and a multispectral drone, following a multi-sensor approach. Object-based classification (for the drone) and pixel-based classification (for satellite images) using the Random Forest algorithm enabled us to map cashew plantations in our study area. The results were then validated based on ground data to identify the strengths and weaknesses of each platform's sensors and provide recommendations for their use. Finally, these findings were discussed to propose a suitable approach for forestry administration to integrate remote sensing data into reference data for agricultural statistics.

2. Study Area

The study was conducted in the Sudanian-Guinean zone, specifically in the municipality of Savè in the Republic of Benin (Figure 1). Savè municipality is located in the central part of Benin in the Collines Department, between 7°41' and 8°20' north latitude and between 2°20' and 2°45' east longitude.

It covers an area of 2228 km² and is divided into eight (08) districts, namely: Besse, Kaboua, Offe, Okpara, Sakin, Adido, Boni, and Savè (which is the district capital). The study area is bounded to the north by the Ouessè municipality, to the south by the Kétou municipality in the Plateau Department, to the west by the Glazoué and Dassa-Zoumè municipalities, and to the east by the states of Oyo, Kwara, and Ogoun in the Federal Republic of Nigeria. Savè, the district capital, is located approximately 255 km from Cotonou. It is crossed by the National Roads RNIE 2 and RNIE 5 (Savè - Oké-Owo).

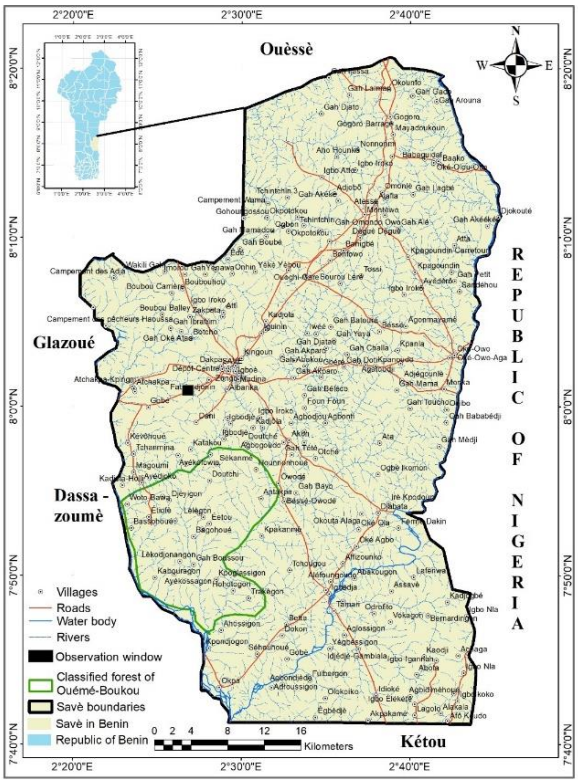

Figure 1. Location of area study

3. Materials and methods

Raster data

The matricial data utilized in this study originated from various aerial platforms, including two different satellites and an Unmanned Aerial Vehicle (UAV) with spatial resolutions ranging from 0.5m (UAV) to 30m (Landsat). The three aerial images from distinct platforms were acquired under similar conditions within a three-day interval during a period of high pressure, ensuring favorable conditions for clear imagery.

The DJI P4 Multispectral (Figure 2) UAV (wingspan: 350 mm, weight: 1487 g, maximum flight duration: 27 minutes, controlled takeoff, and vertical landing) was employed for data collection. It is equipped with a multispectral rotating camera featuring RGB, red, green, blue, near-infrared, and mid-infrared sensors tailored for data acquisition. Shutter speed and sensor sensitivity (ISO)

were manually selected based on brightness conditions. The images were automatically captured once the UAV The integrated autopilot system triggered the camera to cover the scanning area with a 75% overlap. The notable advantage of this sensor's images lies in their very high spatial resolution. However, a drawback is the smaller coverage area of these images, with a smaller swath (a few km), compared to LANDSAT and SENTINEL satellite images, which have swaths of 14400 km and 250 km, respectively reached its scanning area.

Figure 2. UAV multispectral sensor

The Sentinel-2 satellites provide high spatial resolution multi-spectral images, enabling the continuation of data collection from the Landsat and Spot missions while enhancing geometric accuracy for Landsat and repetitiveness for SPOT. Landsat 8 ensures continuous acquisition and availability of Landsat data. It employs a two-sensor payload, namely the Operational Land Imager (OLI) and the Thermal InfraRed Sensor (TIRS). These two instruments respectively capture image data for nine shortwave bands and two thermal bands. Landsat 8 operates in the visible, near-infrared, shortwave infrared, and thermal infrared spectra. The methodology for the approach is shown in figure 3.

Mapping Approach

In summary, our mapping approach revolved around generating a comprehensive and integrated set of inputs from Landsat-8, Sentinel-2, and UAV (Figure 4). The imagery and preprocessed derivatives were compiled for analyses and classification. An assessment of the overall accuracy of the classifications was conducted. Merged imaging observations were introduced into a classifier to map the extent of plantations within the studied observation window. Special attention was given to studying the separability between plantations and other vegetation, as these classes often led to confusion.

Training Data

High-resolution UAV imagery, ground truth data, and high-resolution imagery from Google Earth Pro were combined to create the final polygons. Google Earth Pro contains chronological series of high-resolution data allowing temporal tracking of landscapes on respective dates. Polygons representing different land cover classes were meticulously digitized within the observation window. A range of plantation ages and landscape conditions (i.e., plot size, slope, distance from urban areas) were included to construct a robust validation dataset.

Table 1. Characteristics of different images used for the study

Platform	Types of sensors	Spatial resolution (m)	Spectral band (µm)	Acquisition date	Soleil	
					Az.	Elev.
P4 MULTISPECTRAL	Multispectral	0,5	Red : 0,650 Green : 0,560 Blue : 0,450 RedEdge: 0,730 NIR : 0,840 RGB : 16Mpx	22/07/2023	ND	
SENTINEL 2-A	Multispectral	10	B2–Blue: 0,492 B3–Green: 0,559 B4–Red: 0,664 B8–NIR: 0,832	16/07/2023	ND	
LANDSAT 8 OLI	Multispectral	30	B2 – Blue : 0,450 – 0,515 B3 – Green : 0,525 – 0,600 B4 – Red : 0,630 – 0,680 B5 – NIR : 0,845 – 0,885	21/07/2023	136.37°	48.03°

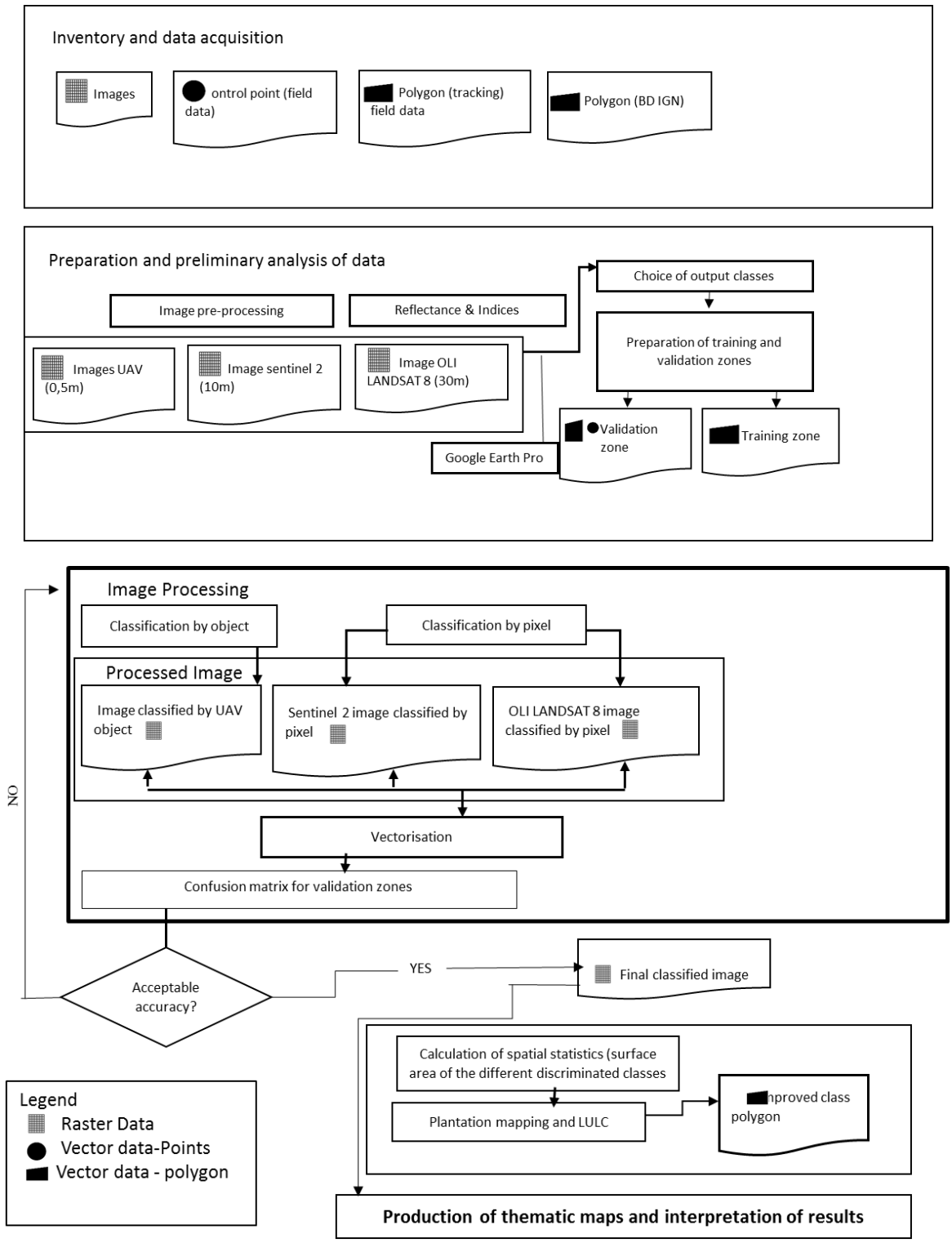

Figure 3. Methodology diagram

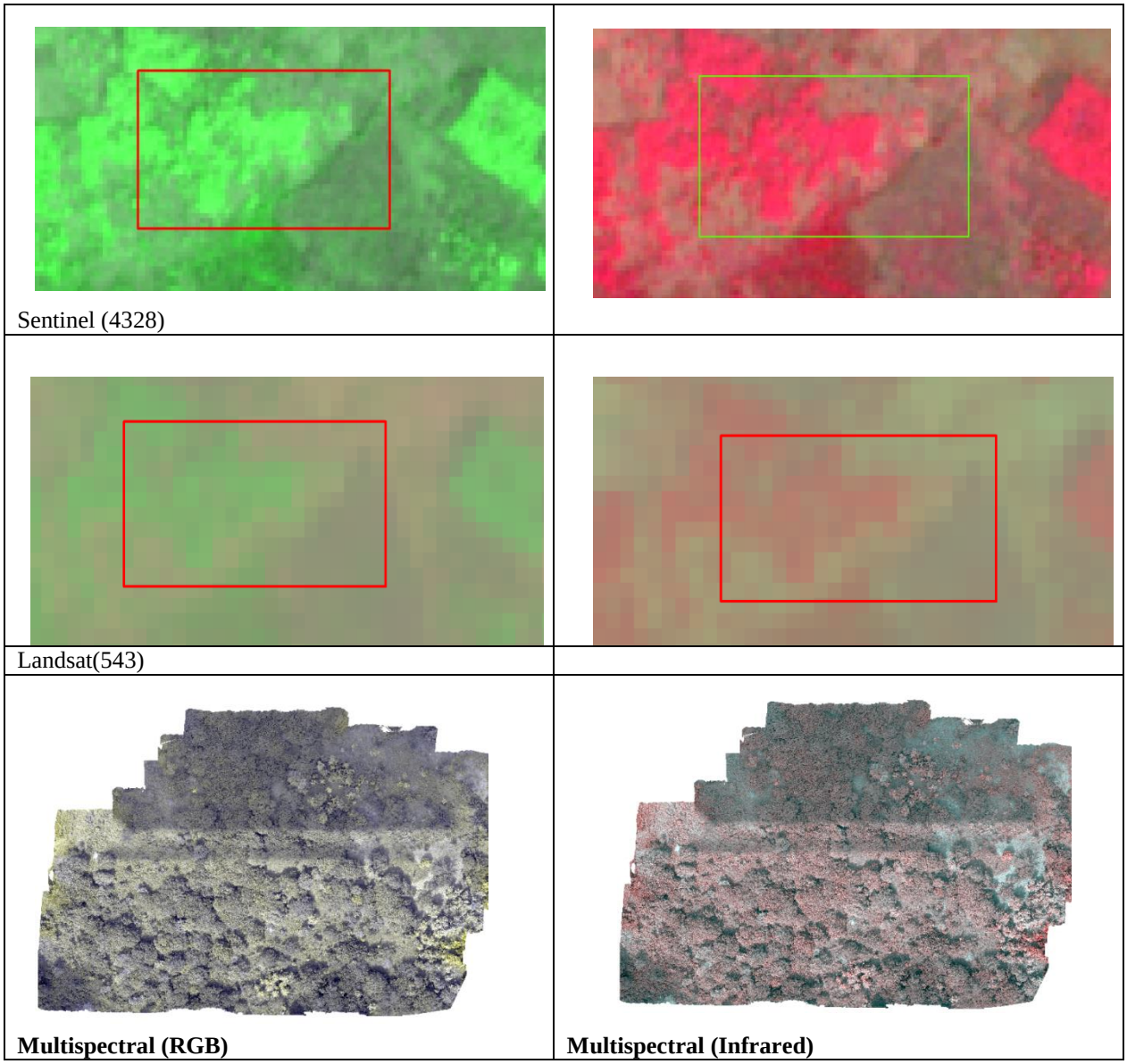

Figure 4. Colour composition and spatial resolution of the different platforms used

The comparison of images from the three different platforms (Landsat, Sentinel, and UAV) yields two (02) observations. The first is related to spatial resolution. The Landsat image has a spatial resolution of 30 meters, implying a resolution three (3) times less precise than the Sentinel image and over thirty (30) times less precise than the UAV image.

Image pre-processing

The process involved geometric and radiometric correction of the matrix data. Radiometric correction aimed to eliminate pixel values not used absolutely but relatively. Regarding geometric correction, GPS data were utilized in conjunction with vector layers of road and hydrographic networks. Additionally, a digital terrain model was generated for ortho-rectification of drone images.

Classification by object

To perform object-based classification of UAV images, Definiens' eCognition software was utilized. The underlying concept of this software is that the semantic information needed to interpret an image is not represented in individual pixels but in meaningful objects and their mutual relationships.

The segmentation process involves dividing an image (Figure 5) into uniform zones (homogeneous objects). It is the process of creating segments (representing objects) with similar characteristics (attributes). The object-based classification method implemented for this work is a supervised classification method based on training zones determined through photo-interpretation. The definition of the homogeneity criterion considers two parameters: color and shape. Color enhancement influences spectral values concerning shape in the homogeneity criterion (Akoguhi et al. 2022). The lower the color criterion, the less spectral homogeneity influences object generation. Shape considers two parameters: compactness and smoothness. This criterion is, in fact, an abstract value (ranging from 0 to 1) that influences the size and shape of the object based on the weighting assigned to each parameter (Akoguhi et al. 2022)

Figure 5. Segmented image (Characteristics: Shape: 0,4; Compactness: 0,5; Scale: 60)

Choice of classes :

The selection of thematic classes is a critical step that significantly influences the results. Indeed, the desired level of detail for extraction has a direct impact on sampling and the validation statistics obtained. The study's targeted objective is the identification of plantations, other vegetation, and cultivated lands. A set of indices, listed below, was also used to assist in the classification within the window. Indices calculated from reflectance data are less sensitive to image noise, geometry, and atmospheric attenuation, making them advantageous, compared to initial reflectance products, in some respects for mapping. This study employed the Normalized Difference Vegetation Index (NDVI; equation (1)) (Rouse et al. 1974; Tucker 1979), a useful measure of landscape greenness and vigor. The Normalized Difference Till Index (NDTI; equation (2)) was used for its sensitivity to residue and leaf moisture as well as crop management practices (Daughtry et al. 2005).

(1) $NDVI = \frac{\rho PIR - \rho R}{\rho PIR + \rho R}$

(2) $NDTI = \frac{\rho swir - \rho swir2}{\rho swir + \rho swir2}$

The Random Forest algorithm was employed (Breiman 2001) to classify remote sensing data for mapping the extent of plantations. Random Forest is a flexible and powerful non-parametric technique that has been recently implemented in numerous mapping applications across various studies, including crop mapping (Lawrence et al. 2014; Watts et al. 2009), wetland mapping (Torbick and Salas 2015; Whitcomb et al. 2009), canopy height mapping (Wilkes et al. 2015), algae proliferation (Song et al. 2015), urban sprawl (Torbick and Salas 2015), biomass (Karlson et al. 2015), and various other thematic domains.

The algorithm creates n trees, each associated with a sample of training data. Each tree then randomly selects m variables and combines them to create the best model. Finally, on new data, each tree predicts a class, and the model predicts the object's class based on a majority vote (Liaw and Wiener 2002).

Whenever a node is split on variable n, the Gini impurity criterion for the two descendant nodes is lower than that of the parent node. Summing the Gini decreases for each individual variable across all trees in the forest provides a quick "importance" measure of the variable, which is often highly consistent with the permutation importance measure. A small value indicates that a node primarily contains observations of a single class.

$Gm = \sum_{k=1}^{k} p_{mk} (1 - p_{mk})$

Où p_{mk} is the proportion of observations of training **k** in the same region **m** that belong to the kth class.

The Gini index is commonly used to measure the purity of nodes. A small value indicates that a node predominantly contains observations from a single class; thus, the Gini index can be used to assess the importance of a particular split.

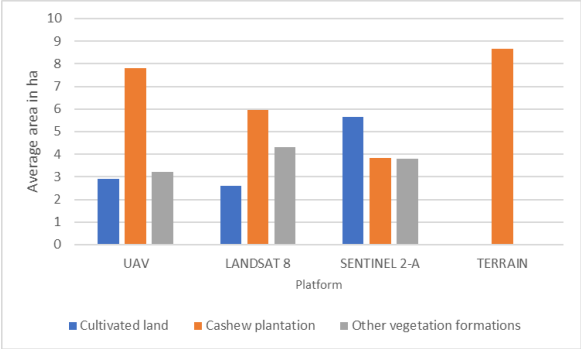

Figure 6. Estimated average surface area per platform

4. Results

Area of classes detected per platform.

The estimated areas of the land-use classes in the test area from the different platforms were extracted in order to compare the results (Figure 6). We note that the areas detected by the different platforms differ from one platform to another; the UAV platform detects a larger area of cashew plantation than the other platforms in our area of investigation, which are respectively around (8 ha) by the UAV; (6 ha) for Landsat; (4 ha) for Sentinel and (around 9 ha) observed in the field (Tracking). The results from these different platforms show that the UAV images are finer than the Sentinel and Landsat images, which confirms the classification results. This is due to the spatial resolution (Goudet 2008).

Field surveys were employed to randomly sample three types of land cover classes (Cashew plantation, cultivated land, and other vegetation formations) for analyzing spectral characteristics. Spectral regions with a higher selection of bands are crucial for detecting and characterizing vegetation due to the distinctively low reflectance in the visible range and high reflectance in the near-infrared (NIR) range. Figure 7 reveals the spectral characteristics of cashew plantations and the stratum of other vegetation formations, which were generally similar and only differed in the infrared region reflectance, with cashew plantations having higher reflectance than the stratum of other vegetation formations (Yujia Chen and Tian 2020) across the three platforms used. In contrast, the spectral characteristics of cultivated lands differed, and their reflectance is lower in the near-infrared compared to other classes (Yujia Chen and Tian 2020).

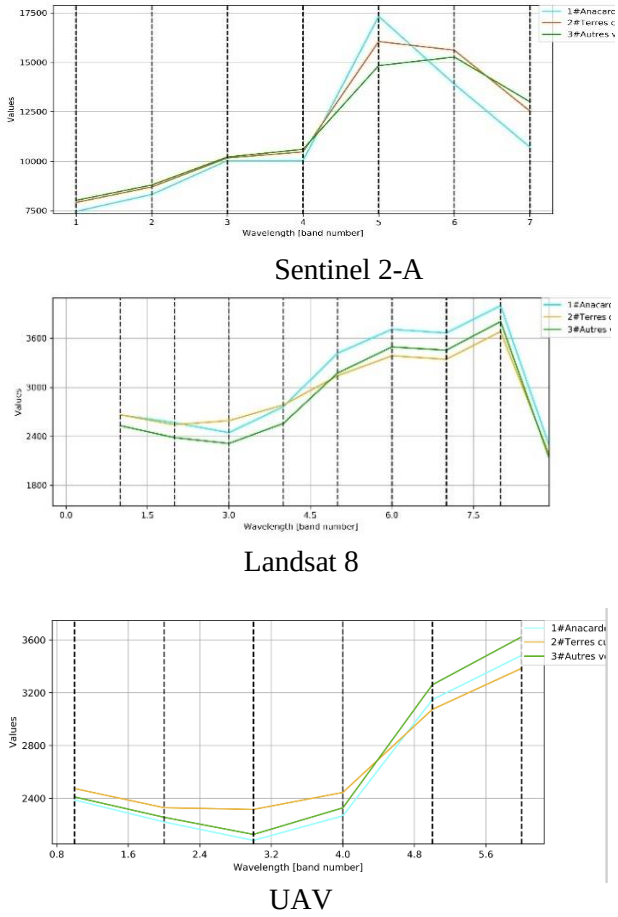

Figure 7. Spectral profiles of thematic units determined globally from the different platforms (LANDSAT, SENTINEL and UAV) in the test area. The y-axis is the mean reflectance value.

Classification, carried out through statistical analyses, was applied to the three classes (cultivated land, cashew plantations, and other vegetation formations) within our area of interest (Figure 7). Following the classification, results obtained with UAV imagery offer a clearer representation of reality compared to Sentinel and Landsat images. However, Sentinel images provide a better depiction of reality compared to Landsat images. Objects that are not visible in Landsat and Sentinel images become discernible, and object boundaries are more defined.

Table 2. Quality assessment indexes for images classified by platform

Platform	Overall accuracy (%)	Kappa index
UAV	82,35	0,72
SENTINEL	65,09	0,48
LANDSAT	47,84	0,23

The results of the classification evaluation using different platforms applied to the study area, comparing the ground truth of labeled test data with the output of the final map, are presented in Table 2. The confusion matrix of the supervised classification from UAV imagery reveals an overall accuracy of 82.35%, with a Kappa coefficient of 0.72 (Table 2). The Sentinel 2 platform shows an accuracy of 65.09% and a Kappa coefficient of 0.48, while Landsat 8 imagery provides an overall accuracy of 47.84% with a Kappa coefficient of 0.23. This demonstrates a superior performance in discriminating land cover classes with the UAV platform compared to the satellite platforms Sentinel and Landsat. However, several confusions occurred during the image classification process. With the UAV platform, the most significant confusions arising from supervised classification were noted between the stratum of other vegetation (0.42). As for the Sentinel platform, more confusions were observed at the level of the cultivated land class (0.24), and with Landsat images, confusions were observed at the level of cultivated land (0.27) and other vegetation formations (0.16).

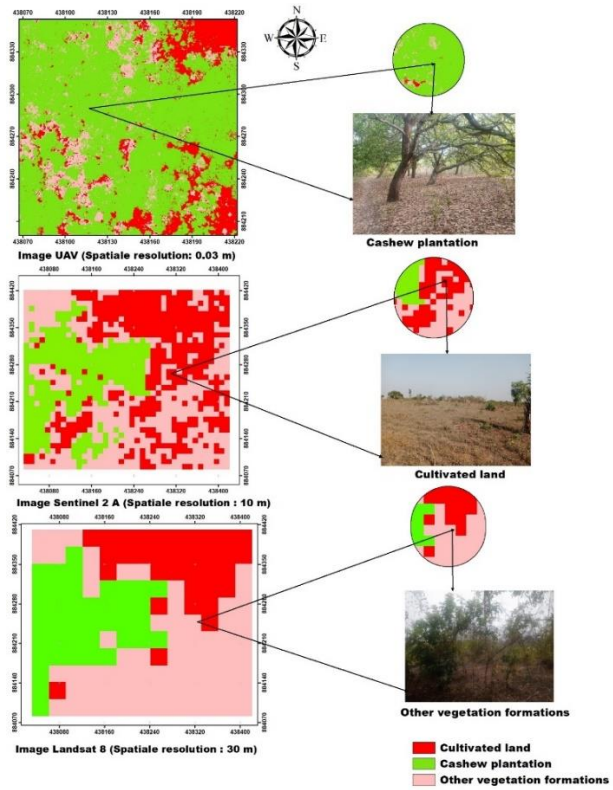

Figure 8. Sample of objects classified using images from different platforms

Across all platforms, the cashew plantation class is well classified, with respective accuracies of 74.16 for UAV, 70.65 for Sentinel, and 77.25 for Landsat (Table 3). This situation could be explained by an intraspecific variation in the spectral signature of the plantation class, which varies depending on their age and tends to be considered as the stratum of other vegetation formations by the algorithm.

These results align with research conducted by (N'guessan et al. 2008) on the satellite remote sensing monitoring of a protected humid tropical forest subject to anthropogenic pressures in the classified forest of Haut Sassandra in Côte d'Ivoire. The confusion matrix highlighted the spectral overlap between cashew plantations and the stratum of other vegetation formations. For Landsat and Sentinel platforms, most pixels of the stratum of other vegetation formations were misclassified as plantations and vice versa.

Table 3. Confusion matrix for images of classified platforms in the study area

Type	Cultivated land	Cashew crop	Others vegetation formations	Commission	User
UAV					
Cultivated land	**104**	1	7	0,07	92,86
Cashew crop	0	**66**	23	0,25	74,16
Others vegetation formations	11	3	**40**	0,25	74,10
Omission	0,09	0,05	0,42		
Producer	90,43	94,28	57,14		
SENTINEL 2-A					
Cultivated land	**53**	1	12	0,19	80,30
Cashew crop	17	**65**	10	0,29	70,65
Others vegetation formations	45	4	**48**	0,50	49,48
Omission	0,24	0,01	0,08		
Producer	75,68	98,03	91,37		
LANDSAT 8					
Cultivated land	**46**	1	11	0,04	95,29
Cashew crop	26	**49**	32	0,22	77,25
Others vegetation formations	43	20	**27**	0,24	75,29
Omission	0,27	0,08	0,16		
Producer	72,94	91,76	83,13		

5. Discussion

Characteristic features of Anacardium occidentale for identification on each platform (satellite and UAV)

The comparative analysis of different platforms (UAV and satellite) allowed for the assessment of their performance in discriminating and characterizing various land cover types in our test area. This methodological approach provided an interpretation of the major land cover categories in the test zone.

Overall, the spectral profiles of the three land cover types in our test area exhibit a distinct spectral behavior in the visible and near-infrared ranges on all platforms (satellite and UAV) used. Vegetated surfaces are characterized by low reflectance in the blue wavelengths, increasing in the green, and again decreasing in the red across images from all platforms. The dip in the curve of other vegetation in the near-infrared (NIR) band (735 nm) may be attributed to the combination of the average spectral signature of species in the other vegetation class, reducing reflectance in the NIR.

Around 735 nm (NIR), the spectral signature curve of cashew plantations shows an increase in reflectance in the NIR wavelengths on satellite platforms. This NIR reflectance in cashew plantations is higher than the overall reflectance of the other vegetation class in the test area. However, on the UAV platform, the reflectance is lower in cashew plantations compared to the stratum of other vegetation in the NIR.

Furthermore, the spectral signature curve of the stratum of other vegetation experiences a drop at a common point in the red band (660 nm), and the curve of Anacardium occidentale (cashew) exhibits a higher ascendancy than the stratum of other vegetation. Specifically, the spectral behavior of Anacardium occidentale stands out from other vegetation due to its higher reflectance compared to other plants, confirming the findings of (Deshayes 2008). Additionally, the reflectance of cultivated lands is lower in the green and NIR bands and higher in the red band compared to other classes, across all platforms (Yujia Chen and Tian 2020).

In conclusion, the results of spectral signatures have helped determine and understand the spectral behavior of land cover units. They have supported the choice of classes in the channels of both satellite and UAV platforms.

Evaluation of the performance of cashew plantation detection and area estimation

The analysis of UAV imagery reveals an overall accuracy of 82.35% and a Kappa index of 0.72. This level of accuracy is significantly higher than the values provided by other platforms, Sentinel (65.09%) and Landsat (47.84%). These results align with (Kosal 2020), who obtained an overall accuracy of 80% and concluded that very high spatial resolution UAV images better capture spatial variability with higher dynamics in vineyard fields. (Matese et al. 2015) also found that UAV imagery is relevant for discriminating small variations in values (better radiometric discrimination) and small spatial structures (better spatial discrimination).

Furthermore, the identification of cashew plantation pixels in the cashew class (user accuracy) by the algorithm was almost similar across all platforms, approximately 77.25% for Landsat, 70.65% for Sentinel, and 74.16% for UAV. This suggests that increased spectral information can partly compensate for coarser spatial resolution (Yin et al. 2023). However, Sentinel data, through the algorithm, showed other vegetation pixels misclassified as agricultural lands and cashew plantations to a lesser extent. This situation is due to fragmentation in certain small regions of the study area, causing satellite platforms (Landsat and Sentinel) to lose their effectiveness. Landsat and Sentinel-2 images cannot adequately represent the boundaries of smallholder cashew plantations, given their spatial resolution, which aligns with observations by (Yin et al. 2023) and (Wang et al. 2022) in their studies on a comparative approach of Sentinel 2 and Landsat 8 for mapping forest species.

The overall pixel analysis of Sentinel and Landsat satellite platforms covering the study area reveals confusion between classes, primarily cashew plantations and the stratum of other vegetation, and to a lesser extent, with cultivated lands. This confirms observations by (Rege et al. 2022), suggesting misclassification by the Random Forest classifier used in land cover classification, utilizing cashew plantation pixels for pixels of other vegetation in the combined dataset of our area of interest.

The high overall accuracy resulting from UAV imagery classification allows us to infer that UAV imagery has a strong detection capability, and UAV data would be highly suitable in complementarity for assessing the spatial distribution of land use types with satellite images to discriminate other land cover classes in a fragmented landscape. Additional sensors or images from higher resolution resources, such as UAV images, could enhance results by providing better spatial representation to discriminate plantations from the "other vegetation" stratum (Koskinen et al. 2019), including additional statistical information such as area.

Moreover, plantation areas were underestimated by satellite platforms, approximately 6 ha for Landsat and 4 ha for Sentinel, compared to UAV imagery, which estimated about 8 ha. Our on-the-ground investigations focused on tracking plantations, resulting in an observed area of 8.67 ha (approximately 9 ha) for cashew plantations. We conclude that the UAV platform provides an estimation of cashew plantation areas close to the observed reality on the ground. Despite similarities in user accuracy among different platforms, uncertainties related to spatial resolution affected overall accuracy and plantation area estimates in Landsat and Sentinel platforms. Certain portions of cashew plantation areas in fragmented zones were underestimated in Landsat and Sentinel images, potentially leading to errors in determining the total plantation area.

The results of this study allow us to deduce, on the one hand, that the automation of cashew plantation detection using optical imagery may pose difficulties between the stratum of other vegetation and plantations because they are spectrally similar and challenging to distinguish using optical satellite imagery (Sentinel and Landsat). Although cashew plantations and other vegetation strata have similar spectral signatures, cashew trees are perennial plants, while the stratum of other vegetation is composed of various species with different characteristics (deciduous and evergreen species), with variable spectral signatures. On the other hand, the use of multi-resolution approaches and the integration of complementary data can contribute to improving the reliability of plantation area estimates through remote sensing.

6. Suggestion

To facilitate the discrimination of a species through remote sensing, we suggest the following points:

- Utilizing multi-temporal data for classification. Increasing the number of dates, along with high-quality images, should enable the acquisition of dates during very specific vegetation periods for the species. Other Sentinel-2 images from non-vegetation periods could assist in creating a mask for the species. (Immitzer et al. 2012) already emphasized the high potential of multi-temporal data for vegetation image classification.
- Improving the quality of reference data (for model training and validation) based on a larger sample of ground-truth data.
- Having access to multi-sensor data to combine different resolutions and spectral and spatial qualities would enhance the quality of segmentation and classification by associating all instantaneous information with the definition of a class.
- Furthermore, the combination of various classifiers based on a priori knowledge could further enhance the method (Yangbo Chen et al. 2017).

7. Conclusions

In this study, we analyzed the uncertainties associated with the detection of cashew plantations and explored how different remote sensing platforms can complement each other in detecting and estimating the areas of cashew plantations. The study successfully identified the species in the test area, leading to a good overall accuracy for the UAV platform compared to satellite platforms (Sentinel and Landsat). However, there is potential for further improvement, especially for the satellite platform, which could benefit from the use of validation data with higher error estimates. The classification results allowed us to discriminate the Anacardium occidentale species in the study area across various aerial imaging platforms and estimate its area.

References:

ACA. (2012). Annual report 2011.

Akoguhi P. N., H. N. Dibi, M. H. Godo, G. N. Adja and F. K. Kouamé (2022). Évaluation des méthodes de classifications dirigées (spectrale et orientée objet) sur les images satellitaires à THRS: Cas de la cartographie du

tissu urbain de la commune de Cocody et d'Attécoubé (Abidjan, Côte d'Ivoire). *VertigO*, (Volume 22 numéro 3). https://doi.org/10.4000/vertigo.36548

Alavipanah S. K., K. Ghazanfari and B. Khakbaz (2010). Remote Sensing and Image understanding as Reflected in Poetical Literature of Iran. http://www.earsel.org/symposia/2010-symposium-Paris/Proceedings/EARSeL-Symposium-2010_1-02.pdf

Alvarez-Vanhard E., T. Corpetti and T. Houet (2021). UAV & satellite synergies for optical remote sensing applications: A literature review. *Science of Remote Sensing*, *3*, 100019. https://doi.org/10.1016/j.srs.2021.100019

Breiman L. (2001). Random Forests. *Machine Learning*, *45*(1), 5–32. https://doi.org/10.1023/A:1010933404324

Chen Y., P. Dou and X. Yang (2017). Improving Land Use/Cover Classification with a Multiple Classifier System Using AdaBoost Integration Technique. *Remote Sensing*, *9*(10), 1055. https://doi.org/10.3390/rs9101055

Chen Yujia and S. Tian (2020). Comparison of pixel- and object-based image analysis for tea plantation mapping using hyperspectral Gaofen-5 and synthetic aperture radar data. *Journal of Applied Remote Sensing*, *14*(04). https://doi.org/10.1117/1.JRS.14.044516

Daughtry G. S. T., J. McmurtreyIII and C. L. Wallthall (2005). Evaluation of Digital Photography from Model Aircraft for Remote Sensing of Crop Biomass and Nitrogen Status, 356–378.

Deshayes M. (2008). *Caractéristiques spectrales des principaux composants de la surface terrestre*. Cours pour Mastère SILAT presented at the Module "Télédétection: Principes de base," UMR TETIS CEMAGREF-CIRAD-ENGREF.

Goudet M. (2008). *Estimation par télédétection de la ressource forestière sur le département du Var* (Mémoire de fin d'Etude de Master) (p. 96). Paris: Agro-Paris-Tech, Engref. https://infodoc.agroparistech.fr/doc_num.php?explnum_id=3342

Immitzer M., C. Atzberger and T. Koukal, T. (2012). Tree Species Classification with Random Forest Using Very High Spatial Resolution 8-Band WorldView-2 Satellite Data. *Remote Sensing*, *4*(9), 2661–2693. https://doi.org/10.3390/rs4092661

Karlson M., M. Ostwald, H. Reese, J. Sanou, B. Tankoano and E. Mattsson (2015). Mapping Tree Canopy Cover and Aboveground Biomass in Sudano-Sahelian Woodlands Using Landsat 8 and Random Forest. *Remote Sensing*, *7*(8), 10017–10041. https://doi.org/10.3390/rs70810017

Kémeuzé V. A., P. M. Mapongmetsem, M. A. Tientcheu, B. A. Nkongmeneck and R. B. Jiofack (2012). Boswellia dalzielii Hutch: State of the stand and traditional use in the Mbé area. *Sécheresse*, *23*(4), 278–283. https://doi.org/10.1684/sec.2012.0365

Kosal K. (2020). *Contribution de l'imagerie dronique pour la caractérisation des paramètres biophysiques des cultures agricoles* (Thèse de Doctorat). Université de Montréal Département de géographie, Faculté des arts et des sciences, Montréal.

Koskinen J., U. Leinonen, A. Vollrath, A. Ortmann, E. Lindquist and R. d'Annunzio. (2019). Participatory mapping of forest plantations with Open Foris and Google Earth Engine. *ISPRS Journal of Photogrammetry and Remote Sensing*, *148*, 63–74. https://doi.org/10.1016/j.isprsjprs.2018.12.011

Lawrence H., J. P. Wigneron, P. Richaume, N. Novello, J. Grant, A. Mialon (2014). Comparison between SMOS Vegetation Optical Depth products and MODIS vegetation indices over crop zones of the USA. *Remote Sensing of Environment*, *140*, 396–406. https://doi.org/10.1016/j.rse.2013.07.021

Liaw A. and M. Wiener (2002). Classification and regression by randomForest. https://cran.r-project.org/doc/Rnews/

Lisein J., A. Michez, H. Claessens and P. Lejeune (2015). Discrimination of Deciduous Tree Species from Time Series of Unmanned Aerial System Imagery. *PLOS ONE*, *10*(11), e0141006. https://doi.org/10.1371/journal.pone.0141006

Matese A., P. Toscano, S. Di Gennaro, L. Genesio, F. Vaccari, J. Primicerio (2015). Intercomparison of UAV, Aircraft and Satellite Remote Sensing Platforms for Precision Viticulture. *Remote Sensing*, *7*(3), 2971–2990. https://doi.org/10.3390/rs70302971

N'guessan E., H. Dibi N'da, M. F. Bellan and F. Blasco (2008). Pression anthropique sur une réserve forestière en Côte d'Ivoire : Apport de la télédétection, *5 (4)*, 307–323.

Queinnec M., J. C. White and N.C. Coops (2021). Comparing airborne and spaceborne photon-counting LiDAR canopy structural estimates across different boreal forest types. *Remote Sensing of Environment*, *262*, 112510. https://doi.org/10.1016/j.rse.2021.112510

Rege A., S. B. Warnekar and J. S. H. Lee (2022). Mapping cashew monocultures in the Western Ghats using optical and radar imagery in Google Earth Engine. *Remote Sensing Applications: Society and Environment*, *28*, 100861. https://doi.org/10.1016/j.rsase.2022.100861

Rouse J., J. Haas, J. Schell and D. Deering (1974). Monitoring vegetation systems in the Great Plains with ERTS. In Proceedings of the Third ERTS Symposium, . 309-317.

Saadou M. (1999). Evaluation de la biodiversité biologique au Niger : éléments constitutifs de la biodiversité végétale. Conseil National de l'Environnement pour un Développement Durable SE/CNEDD.

Song W., J. Dolan, D. Cline and G. Xiong (2015). Learning-Based Algal Bloom Event Recognition for Oceanographic Decision Support System Using Remote Sensing Data. *Remote Sensing*, *7*(10), 13564–13585. https://doi.org/10.3390/rs71013564

Tandjiékpon (2010). Analyse de la chaine de valeur du secteur anacarde du Bénin.

Torbick N. and W. Salas (2015). Mapping agricultural wetlands in the Sacramento Valley, USA with satellite remote sensing. *Wetlands Ecology and Management*, *23*(1), 79–94. https://doi.org/10.1007/s11273-014-9342-x

Tucker C. J. (1979). Red and photographic infrared linear combinations for monitoring vegetation. *Remote Sensing of Environment*, *8*(2), 127–150. https://doi.org/10.1016/0034-4257(79)90013-0

Wang M., Y. Zheng, C. Huang, R. Meng, Y. Pang, W. Jia (2022). Assessing Landsat-8 and Sentinel-2 spectral-temporal features for mapping tree species of northern plantation forests in Heilongjiang Province, China. *Forest Ecosystems*, *9*, 100032. https://doi.org/10.1016/j.fecs.2022.100032

Watts J. D., R. L. Lawrence, P. R. Miller and C. Montagne (2009). Monitoring of cropland practices for carbon sequestration purposes in north central Montana by Landsat remote sensing. *Remote Sensing of Environment*, *113*(9), 1843–1852. https://doi.org/10.1016/j.rse.2009.04.015

Whitcomb J., M. Moghaddam, K. McDonalds E. Podest and J. Kellnorfer (2009). Mapping vegetated wetlands of Alaska using L-band radar satellite imagery, 54–72.

Wilkes P., S. Jones, L. Suarez, A. Mellor, W. Woodgate, M. Soto-Berelov (2015). Mapping Forest Canopy Height Across Large Areas by Upscaling ALS Estimates with Freely Available Satellite Data. *Remote Sensing*, *7*(9), 12563–12587. https://doi.org/10.3390/rs70912563

Yin L., R. Ghosh, C. Lin, D. Hale, C. Weigl, J. Obarowski (2023). Mapping smallholder cashew plantations to inform sustainable tree crop expansion in Benin. https://www.researchgate.net/publication/366821970_Mapping_smallholder_cashew_plantations_to_inform_sustainable_tree_crop_expansion_in_Benin

Zhang J. (2010). Multi-source remote sensing data fusion: status and trends. *International Journal of Image and Data Fusion*, *1*(1), 5–24. https://doi.org/10.1080/19479830903561035